

# Fiber metallic glass laminates

B.A. Sun

*Institute of Physics, Chinese Academy of Sciences, Beijing 100190, People's Republic of China; and Department of Mechanical Engineering, The Hong Kong Polytechnic University, Hong Kong, People's Republic of China*

K.P. Cheung, J.T. Fan, and J. Lu<sup>a)</sup>

*Department of Mechanical Engineering, The Hong Kong Polytechnic University, Hong Kong, People's Republic of China*

W.H. Wang<sup>b)</sup>

*Institute of Physics, Chinese Academy of Sciences, Beijing 100190, People's Republic of China*

(Received 2 December 2009; accepted 4 January 2010)

The fabrication and properties of fiber metallic glass laminates (FMGL) composite composed of Al-based metallic glasses ribbons and fiber/epoxy layers were reported. The metallic glass composite possesses structural features of low density and high specific strength compared to Al-based metallic glass and crystalline Al alloys. The material shows pronounced tensile ductility compared to monolithic bulk metallic glasses.

## I. INTRODUCTION

The design of modern high-performance structural engineering materials is driven by optimizing combinations of mechanical properties such as strength, ductility, toughness, and elasticity.<sup>1</sup> Composites, by incorporating two or more phases in a material, often possess unique properties that are not attainable by either of the constituents acting alone.<sup>2</sup> Metallic glasses, as a new class of materials, have unique mechanical properties compared to their crystalline counterparts.<sup>3–5</sup> However, their applicability as structural materials is limited by their glass-forming ability (GFA) and poor ductility. At room temperature, bulk metallic glasses (BMGs) often deform inhomogeneously with severe plastic strains localized in narrow shear bands that propagate fast to cause catastrophic failure, which often makes them exhibit limited compressive plasticity and near-zero tensile ductility.<sup>6–8</sup> The natural way to improve the plasticity of BMGs is to fabricate BMG composites by in/ex situ introducing crystalline phases into the glass matrix.<sup>9,10</sup> Carbon has been found to be effective for improving the mechanical and physical properties of BMGs.<sup>11,12</sup> It is reported that significant tensile ductility and good fatigue resistance can be achieved by delicately adjusting the microstructure length scales in BMG composites.<sup>13</sup> While the strategy requires that the BMGs used have good GFA and high processibility during casting, only limited compositions are available.

Fiber metal laminates (FML), as a family of new hybrid composites, consist of bonded thin metal sheets (e.g., Al alloys) and fiber/adhesive layers.<sup>14</sup> This laminated structure, which provides material with excellent fatigue, impact, and damage tolerance characteristics and a low density, has been widely used as aircraft structures.<sup>14–16</sup> In this work, we report the formation of fiber metallic glass laminates (FMGL) composite, which is composed of Al-based metallic glass layers and carbon fiber/epoxy layers. The composite exhibits high tensile strength up to 760 MPa and low density, which grant it higher specific strength and good ductility both under tensile and bending conditions.

## II. EXPERIMENTAL

Al<sub>86</sub>Ni<sub>9</sub>La<sub>5</sub> alloy ingots with nominal composition were prepared by arc melting the mixtures of pure elements in a Ti-gettered Ar atmosphere. Metallic glass ribbons with a thickness of about 30 μm and width of 7 mm were steadily obtained using the single roller melt spinning technique. The amorphous nature of both as-cast and laminated ribbons was ascertained by x-ray diffraction and differential scanning calorimetry methods. The unidirectional carbon fiber prepregs (supplied by GuangWei Composite, Beijing, China, epoxy 40% wt) were 7 mm in width and 50 μm in thickness. Twenty-ply Al<sub>86</sub>Ni<sub>9</sub>La<sub>5</sub> glassy ribbons and 19-ply carbon fiber layers were stacked alternately with ribbons aligned along the direction of carbon fibers. The laminated composite was then cured at 130 °C for 4 h under a pressure of 0.5 MPa, as illustrated in Fig. 1(a). The final laminated composite had a size of 75 mm × 7 mm × 1.2 mm [Fig. 1(b)]. [There is a difference between the predicted thickness of the sample

Address all correspondence to these authors.

<sup>a)</sup>e-mail: mmmelu@inet.polyu.edu.hk

<sup>b)</sup>e-mail: whw@aphy.iphf.ac.cn

DOI: 10.1557/JMR.2010.0291

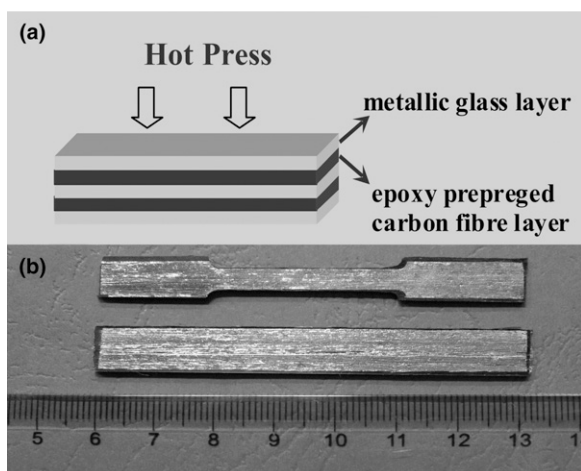


FIG. 1. (a) Schematic illustrations of the fabrication of FMGL and (b) photographs of the ultimate FMGL samples.

(1.55 mm) and the actual thickness, because some epoxy was squeezed out of the structure during pressing/curing.] The uniaxial tensile and three-point bending tests were conducted at room temperature using an Instron electro-mechanical 3384 test system (Norwood, MA) at a strain rate of  $2 \times 10^{-4} \text{ s}^{-1}$  and displacement rate of  $0.5 \text{ mm min}^{-1}$ , respectively. The samples for the tensile test were first ground carefully into a dog bone shape, and then bonded to four Al alloy sheets with epoxy at both ends in case of the clamp effect occurring during the tests. The uniaxial elongation of the sample in the tensile test was measured by an extensometer with a gauge length of 25 mm. The normal strain was then determined by the division of the elongation by the length between the measuring points under no loading. In this study, the normal (engineering) stress–strain curves were used. The Young’s modulus of the sample was roughly determined from the linear regime (in the strain range of  $0 \sim 0.5\%$ ) of tensile stress–strain curves, as the elastic part of the curve was not perfectly straight. The support span for three-point bending is 2 mm. The morphologies of specimens were observed using a Philips XL 30 scanning electron microscope (SEM; Eindhoven, The Netherlands). The density was measured using the Archimedeian technique with an accuracy of 1.0%.

### III. RESULTS AND DISCUSSIONS

Figure 2 shows the cross section of the laminated structure of the composite. The fiber/epoxy layers and  $\text{Al}_{86}\text{Ni}_9\text{La}_5$  metallic glass layers are alternately stacked [Fig. 2(a)]. The contrast of cross section of carbon fibers embedded in epoxy can be clearly seen in Fig. 2(b). After being epoxy cured, there are no holes and gaps at the interface [Fig. 2(b)] and the glassy layers and fiber layers are well bonded. The average thickness of glass layers and fiber layers estimated from Fig. 2(a) is 29 and 40  $\mu\text{m}$ ,

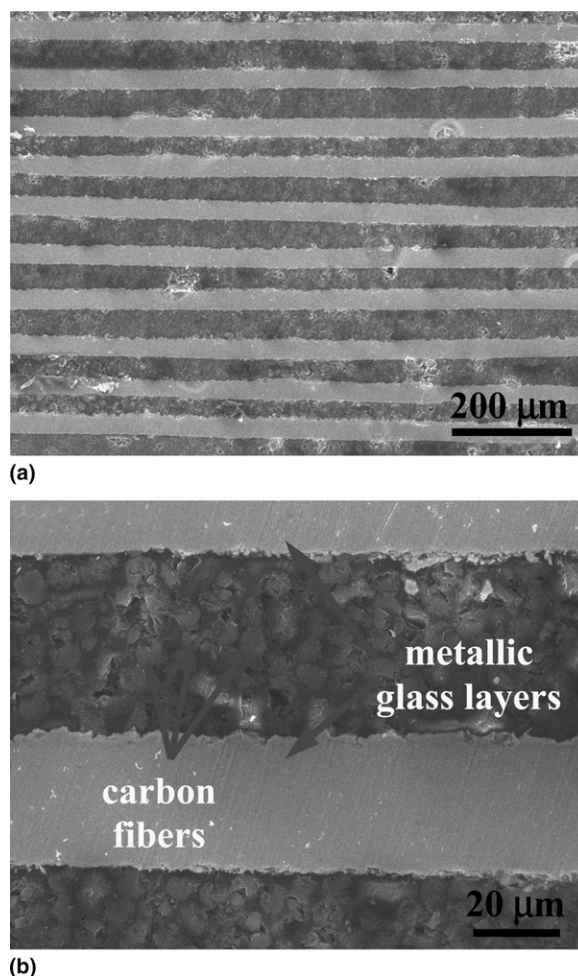


FIG. 2. (a) Typical SEM micrograph for the cross section of FMGL and (b) magnified graph that shows the clear contrast for carbon fibers.

respectively. The volume fractions for the two phases are estimated to be 42% and 58%, respectively.

The  $\text{Al}_{86}\text{La}_5\text{Ni}_9$  metallic glass ribbons, although showing good bending ductility, exhibited poor tensile ductility. After about 1% elastic elongation in the tensile stress–strain curve [Fig. 3(a)], the ribbon fractured catastrophically with strength of about 680 MPa. The fracture strength is far lower than that of reported Al-based metallic glass ribbons,<sup>17</sup> which may be due to the edge defects that formed during melt spinning. The fiber reinforced composite (FRC), which consists of carbon fiber/epoxy layers alone, showed a high fracture strength of about 900 MPa [Fig. 3(a)] but zero plastic strains under tensile conditions. The fiber metallic glass laminates, however, exhibited obvious plastic elongation (about 2%) in the tensile stress–strain curve, as shown in Fig. 3(a), which is better than its constituent phases. However, it had a strength of about 760 MPa, which is slightly lower than those of reported Al-based metallic glass ribbons and FRC, but greatly exceeds the highest value (530 MPa) obtained in optimal age-hardened Al commercial

alloys.<sup>18</sup> After the sample fractured, most fiber layers were separated from the metallic glass layers and the fiber bundles were also dispersed [see inset of Fig. 3(a)], suggesting the delamination at the interfaces as often occurs in FML,<sup>19</sup> which is the dominant failure mode for FMGL under tensile conditions. In addition, FMGL has excellent bending ductility compared with FRC. Figure 3(b) shows the flexural stress–strain curves of FMGL and FRC. The flexural stress  $\sigma_f$  and flexural

strain  $\varepsilon_f$  are given by  $\sigma_f = 3PL/2bd^2$ ,  $\varepsilon_f = 6Dd/L^2$  for a rectangular cross section,<sup>20</sup> where  $P$  is the bending load,  $D$  is the bending displacement at the midpoint of the sample,  $L$  is the support span, and  $b$ ,  $d$  are the width and depth of the test sample, respectively. The flexural strength for FMGL is about 610 MPa, lower than that of FRC. However, the stable flexural strain (the strain before which the flexural stress can sustain a rough platform) can reach 6%, which is much better than that of FRC (2%). It is noted that the delamination did not occur when the sample failed, which is different from what happened in the tensile test, suggesting that the interfaces between metallic glass and fiber layers behave more strongly under bending conditions.

Table I summarizes some physical and mechanical properties of FMGL, as well as some commercial Al alloys and monolithic metallic glasses. It can be seen that FMGL has a much reduced density (1.86 g/cm<sup>3</sup>), compared to Al-based metallic glasses and Al commercial alloys, which can be attributed to the presence of the much lighter fiber/epoxy phase. The measured density for FMGL is lower than the calculated density (2.15 g/cm<sup>3</sup>) based on the rules of mixture in composite materials ( $\rho = \sum f_i \rho_i$ , where  $f_i$  and  $\rho_i$  are the volume fraction and density for the  $i$ th phase, and the measured density for the metallic glass phase and fiber plus epoxy phase are 3.26 g/cm<sup>3</sup> and 1.41 g/cm<sup>3</sup>, respectively). This density discrepancy suggests that the two constitute phases in FMGL are not in an ideally bonded state and there may exist some microholes in the epoxy phase due to the gas emission in the process of curing. Due to the low density, the specific strength defined by the ratio of strength to density for FMGL reaches  $4.09 \times 10^5$  Nm kg<sup>-1</sup>, which exceeds the values obtained from Al-based metallic glasses, Zr-based BMGs, and Al commercial alloys (ranges from  $1.8 \times 10^5$  to  $3.45 \times 10^5$  Nm kg<sup>-1</sup>). The specific strength defined by the ratio of yielding strength to the density for FMGL is also high ( $2.15 \times 10^5$  Nm kg<sup>-1</sup>), larger than those of materials (Refs. 21–25) that have obvious plastic strains listed in Table I.

To shed light on the deformation mechanism of FMGL, the micrographs of the fracture surface for the tensile sample are shown in Fig. 4. The delamination can

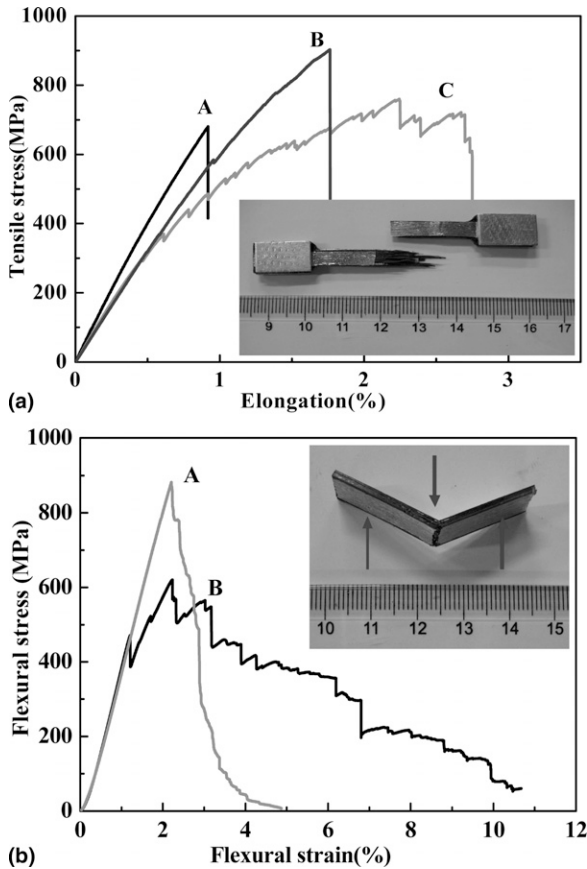


FIG. 3. (a) Uniaxial tensile stress–strain curves for Al<sub>86</sub>Ni<sub>9</sub>La<sub>5</sub> glassy ribbon (A), FRC (B), and FMGL (C), respectively. The inset is the photograph of the failed FMGL sample. (b) The flexural stress–strain curves for FMC (A) and FMGL (B) obtained from three-point bending tests. The inset is also the photograph of the FMGL sample failed in three-point bending.

TABLE I. Mechanical and physical properties for different classes of materials, including density  $\rho$ , Young’s modulus  $E$ , the yielding strength  $\sigma_y$ , fracture strength  $\sigma_f$ , tensile plastic elongation  $\varepsilon_p$ , and specific strength  $\sigma_p$  defined by the ratio of fracture strength to the density.

Materials	$\rho$ (g/cm <sup>3</sup> )	$E$ (GPa)	$\sigma_y$ (MPa)	$\sigma_f$ (MPa)	$\varepsilon_p$ (%)	$\sigma_p$ (10 <sup>3</sup> Nm.kg <sup>-1</sup> )	Reference
FMGL	1.86	70.7	~400	760	~2	409	This work
Al <sub>86</sub> Ni <sub>9</sub> La <sub>5</sub> glassy ribbon	3.26	75.0	680	680	0	209	This work
Al <sub>87</sub> Ni <sub>5</sub> Y <sub>8</sub> glassy ribbon	3.30	71.2	1140	1140	0	345	17
Zr <sub>47.5</sub> Cu <sub>47.5</sub> Al <sub>5</sub> BMG	7.195	88.7	2000	2265	0	315	21
Zr <sub>64.13</sub> Cu <sub>15.75</sub> Ni <sub>10.12</sub> Al <sub>10</sub> BMG	6.604	78.4	1690	1690	0	256	22
Al alloy 7075-T6	2.85	71	480	510~538	5~8	~180	23
Carbon fiber-T300	1.74	230	3500	3500	~0	2011	24
GLARE (FML)	~2.3	58	283~305	716	~4.7	311	25

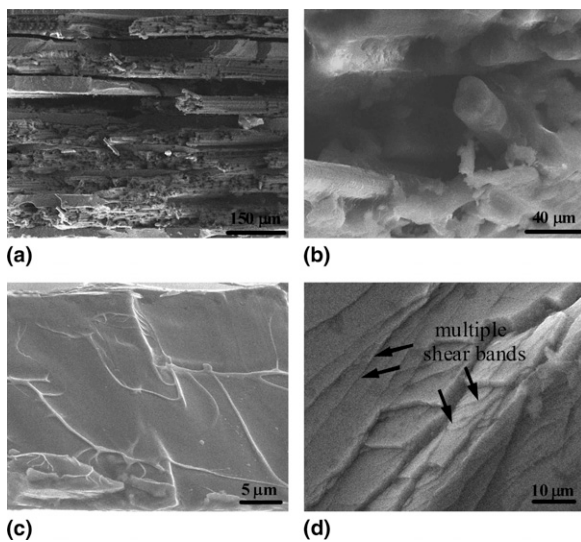


FIG. 4. (a) Typical micrographs of fracture surface of FMGL after the uniaxial test in large scale. One can clearly see the laminate structure; (b) fracture appearance of fiber/epoxy layer in FMGL; (c) fracture appearance of the metallic glass layer in FMGL; (d) side view of the delaminated glassy ribbon near the fracture region.

be clearly seen at the interfaces between the metallic glass and fiber/epoxy layers from the fracture surface [Fig. 4(a)]. However, the fibers are not separated from the epoxy after the sample failed as shown in Fig. 4(b). In addition, the river patterns can be seen from the fracture surface of the metallic glass layer in FMGL [Fig. 4(c)], which is often observed in the fracture of ductile metallic glasses.<sup>26,27</sup> Moreover, multiple shear bands can also be observed from the side of delaminated glassy layers near the fracture regions [Fig. 4(d)]. All the markings indicate that the glassy layers in FMGL were subjected to significant plastic deformation before the sample failed. Generally, monolithic glassy ribbons generally exhibit zero plastic strain in tensile tests; especially in the presence of edge defects.<sup>17</sup> The cracks will be initiated from these defects and rapidly propagate under unconstrained load conditions. However, the glassy ribbons laminated and confined with fiber layers are in a complex stress state during the deformation. The propagation of cracks in the glassy ribbons could be constrained by the complex stress states even if the globe FMGL is under a tensile load, and then plastic yielding occurs at the crack tips. Because the FRC has higher strength than the metallic glass ribbon, the high loads in FMGL during deformation will first induce the plastic yielding of the metallic glass layers, which redistributes the high stresses in-plane in the metallic glass layer to a large area, but also in the thickness direction into the fiber layers. The load transfer to fiber layers prohibits premature failure, but induces shear stresses at the interface, resulting in delamination.<sup>19</sup> In addition, the fatigue behavior is often greatly enhanced due to the unique balance between delamination

at the interfaces and crack growth in the metal layers for FML during cyclic loading.<sup>14,19</sup> Therefore, excellent fatigue resistance is expected for the FMGL.

Inducing structural inhomogeneity is an effective approach to ductilize BMG and BMG-based composites.<sup>11,22,28</sup> This kind of structure often consists of micro- or nano-scale regions with different elastic/plastic properties (soft and hard regions<sup>22</sup>). The soft region can facilitate shear band initiation, while the hard regions can effectively impede shear bands from propagating catastrophically. The interaction between soft/hard regions would induce the formation and branching/arresting of multiple shear bands, accommodating more inelastic strain. The plasticity enhancement in FMGL can also be explained by the soft–hard model. The metallic glassy phase, which will yield first in the deformation, can be viewed as “soft regions” in FMGL. The shear bands initiated in metallic glassy layers will effectively be arrested by the fiber layers (hard regions). On the other hand, the high stress in the fiber layer will also be relaxed by the yielding of glassy layers. The synergy and interaction between the glassy layers and fiber layers is responsible for the pronounced tensile ductility in FMGL. In addition, the mechanical properties of FMGL can gradually change by tuning the arrangement of the fiber and metallic glassy layers such as the volume fraction of two phases, the thickness of fiber layers, and so on. Therefore, in FMGL the soft and hard regions are controllable.

#### IV. CONCLUSIONS

We obtained the fiber metallic glass laminates composite composed of Al-based metallic glasses ribbons and fiber/epoxy layers. The fabrication and formation of the novel alloys are investigated. The metallic glass composite possesses structural features of low density and high specific strength compared to Al-based metallic glass and crystalline Al alloys. The material shows pronounced tensile ductility compared to monolithic BMGs. The strategy might have implications for the future search of tough metallic material.

#### ACKNOWLEDGMENTS

The authors are grateful to the financial support of the Natural Science Foundation of China (Nos. 50890171, 50731008, and 50921091) and Ministry of Science and Technology of China (MOST) 973 (No. 2007CB613904) and Research Grants Council of Hong Kong Special Administrative Region of China under PolyU 5203/08E and PolyU/CRF/08.

#### REFERENCES

1. M.F. Ashby: *Materials Selection in Mechanical Design* (Pergamon, Oxford, UK, 1992).

2. R.A. Donald: *The Science and Engineering of Materials* (Brooks/Cole Engineering Division, Monterey, CA, 1984), Chap. 16.
3. W.H. Wang: Bulk metallic glasses with functional properties. *Adv. Mater.* **21**, 4524 (2009).
4. A.L. Greer: Metallic glasses. *Science* **267**, 1947 (1995).
5. W.H. Wang: The correlation between the elastic constants and properties in bulk metallic glasses. *J. Appl. Phys.* **99**, 093506 (2006).
6. C.A. Schuh, T.C. Hufnagel, and U. Ramamurty: Mechanical behavior of amorphous alloys. *Acta Mater.* **55**, 4067 (2007).
7. C.A. Pampillo: The strength and fracture characteristics of Fe, Ni-Fe and Ni-base glasses. *J. Mater. Sci.* **10**, 1194 (1975).
8. W.J. Wright, R. Saha, and W.D. Nix: Deformation mechanisms of the  $Zr_{40}Ti_{14}Ni_{10}Cu_{12}Be_{24}$  bulk metallic glass. *Mater. Trans.* **42**, 642 (2001).
9. C.C. Hays, C.P. Kim, and W.L. Johnson: Microstructure controlled shear band pattern formation and enhanced plasticity of bulk metallic glasses containing in situ formed ductile phase dendrite dispersions. *Phys. Rev. Lett.* **84**, 2901 (2000).
10. D.H. Bae, D.H. Kim, and D.J. Sordelet: Synthesis of Ni-based bulk metallic glasses by warm extrusion of powders. *Appl. Phys. Lett.* **83**, 2312 (2003).
11. W.H. Wang, Q. Wei, and H.Y. Bai: Enhanced thermal stability and microhardness in metallic glass ZrTiCuNiBe alloys by carbon addition. *Appl. Phys. Lett.* **71**, 58 (1997).
12. Z. Bian, M.X. Pan, Y. Zhang, and W.H. Wang: Carbon-nanotube-reinforced  $Zr_{52.5}Cu_{17.9}Ni_{14.6}Al_{10}Ti_5$  bulk metallic glass composites. *Appl. Phys. Lett.* **81**, 4739 (2002).
13. D.C. Hofmann, J.Y. Suh, A. Wiest, G. Duan, M.L. Lind, M.D. Demetriou, and W.L. Johnson: Designing metallic glass matrix composites with high toughness and tensile ductility. *Nature* **451**, 1085 (2008).
14. C.A. Vermeeren: An historic overview of the development of fiber metal laminates. *Appl. Compos. Mater.* **10**, 189 (2003).
15. L.B. Vogelesang and A. Volt: Development of fibre metal laminates for advanced aerospace structures. *J. Mater. Process. Technol.* **103**, 1 (2000).
16. A. Volt, L.B. Vogelesang, and T.J. Vries: Development of fibre metal laminates for advanced aerospace structures. *Aircr. Eng. Aerosp. Tec.* **71**, 558 (1999).
17. A. Inoue: Amorphous, nanoquasicrystalline and nanocrystalline alloys in Al-based systems. *Prog. Mater. Sci.* **43**, 365 (1998).
18. *Metals Databook*, edited by Japan Institute of Metals (Maruzen, Tokyo, 1983).
19. R.C. Alderliesten: Damage tolerance of bonded aircraft structures. *Int. J. Fatigue* **31**, 1024 (2009).
20. ASTM D790. Test methods for flexural properties of unreinforced and reinforced plastics and electrical insulating materials, in *Annual Book of ASTM Standards*, Vol. 08.01 (ASTM International, West Conshohocken, PA, 2003).
21. P. Yu and H.Y. Bai: Anomalous compositional dependence of Poisson's ratio and plasticity in CuZrAl bulk metallic glasses. *Mater. Sci. Eng., A* **485**, 1 (2008).
22. Y.H. Liu, G. Wang, R.J. Wang, D.Q. Zhao, M.X. Pan, and W.H. Wang: Super plastic bulk metallic glasses at room temperature. *Science* **315**, 1385 (2007).
23. Y.H. Zhao, X.Z. Liao, Z. Jin, R.Z. Valiev, and Y.T. Zhu: Microstructures and mechanical properties of ultrafine grained 7075 Al alloy processed by ECAP and their evolutions during annealing. *Acta Mater.* **52**, 4589 (2004).
24. S. Kumar: Advanced materials: Challenge next decade, in *Proc. Znt. SAMPE Symp. and Exhib.*, edited by G. Janicki, V. Bailey, and H. Schjelderup, Vol. 35 (Cambridge, UK, 1990), p. 2224.
25. The Aluminium Association, Standard and Data (2005).
26. X.K. Xi, D.Q. Zhao, M.X. Pan, W.H. Wang, Y. Wu, and J.J. Lewandowski: Fracture of brittle metallic glasses: Brittleness or plasticity. *Phys. Rev. Lett.* **94**, 125510 (2005).
27. G. Wang, D.Q. Zhao, H.Y. Bai, M.X. Pan, A.L. Xia, B.S. Han, X.K. Xi, Y. Wu, and W.H. Wang: Nanoscale periodic morphologies on fracture surface of brittle metallic glasses. *Phys. Rev. Lett.* **98**, 235501 (2007).
28. J.G. Wang, D.Q. Zhao, M.X. Pan, and W.H. Wang: Mechanical heterogeneity and mechanism of plasticity of metallic glasses. *Appl. Phys. Lett.* **94**, 031904 (2009).